Proceedings of the ASME 2021 16th International Manufacturing Science and Engineering Conference
MSEC2021
June 21-25, 2021, Virtual, Online

MSEC2021-1880

DESIGNING AN INTERCHANGEABLE MULTI-MATERIAL NOZZLE SYSTEM FOR 3D BIOPRINTING PROCESS

Cartwright Nelson
Department of Sustainable Product Design and Architecture, Keene State College, Keene, NH.

Slesha Tuladhar
Department of Sustainable Product Design and Architecture, Keene State College, Keene, NH.

Md Ahasan Habib, Ph.D.
Department of Sustainable Product Design and Architecture, Keene State College, Keene, NH.

ABSTRACT

Three-dimensional bioprinting is a rapidly growing field attempting to recreate functional tissues for medical and pharmaceutical purposes. Development of functional tissue requires deposition of multiple biomaterials encapsulating multiple cell types i.e. bio-ink necessitating switching ability between bio-inks. Existing systems use more than one print head to achieve this complex interchangeable deposition, which decreases efficiency, structural integrity, and accuracy. In this research, we developed a nozzle system capable of switching between multiple bio-inks with continuous deposition ensuring the minimum transition distance so that precise deposition transitioning can be achieved. Finally, the effect of rheological properties of different bio-material compositions on the transition distance is investigated by fabricating the sample scaffolds.

Keywords: Multi-material, 3D bio-printing, rheology, nozzle system.

1. INTRODUCTION

Bioprinting is an emerging field that has the potential to recreate 3D functional living tissue by allocating biomaterials along with high precision positioning of cells in a layer-by-layer fashion [1, 2]. Among various techniques, the extrusion-based 3D bioprinting technique can fabricate intricate and well-defined pore geometries with a single or multiple materials mimicking the native tissue architecture [3]. Due to various factors such as biocompatibility, less cytotoxicity, and high-water content (<90%), hydrogels extracted from nature are commonly considered as the bio-ink for scaffold fabrication in extrusion-based bio-printing technique [4].

Success in tissue engineering depends on the ability to fabricate the scaffold mimicking the native tissue architecture with controlled deposition of multiple bio-materials encapsulating multiple cells [5]. Various efforts have been reported to fabricate tissue scaffold using multi-materials and cell types [6-8]. A multi-head tissue/organ building system (MtoBS) was designed to fabricate scaffolds with polycaprolactone (PCL) and alginate with different cell types [9]. Another multi-head deposition technique was designed to fabricate a mechanically strong scaffold with synthetic polymers [10]. An Integrated Organ Printing (IOP) system consisting of multiple cartridges was used to fabricate the structure of natural urethra of rabbits ensuring mechanical properties and better cell growth. Some other works have also been reported where multiple print heads have been used to fabricate multi-material scaffolds [11-14]. However, fabricating the scaffold with multiple materials often involves the sequential deposition of different materials. Each material deposited needs to carefully align with the subsequent nozzle and routinely create a flow of bio-ink on-demand with a lot of interruption. All of this must be done precisely, without introducing defects. Therefore, multi-head 3D bioprinters have some inherent drawbacks which increase fabrication time due to switching between multiple materials [15-17]. Moreover, switching between materials creates discontinuity which reduces the shape fidelity and eventually undermines the mechanical integrity of the final scaffold [15]. In this research, we have developed a nozzle system capable of switching between multiple hydrogels with continuous deposition through the same nozzle outlet, ensuring the minimum transition distance so that precise deposition transitioning can be achieved.

The flowability of the biomaterials, and ability to form and hold filament geometry i.e. printability, can be controlled by the rheology of the considered biomaterials [25, 26]. The viscosity of the biomaterials, which can be increased by increasing the solid content [29-31], directly impacts the printability and shape fidelity of the filament and final scaffold [27, 28]. It can also affect the transition distance for multi-material deposition [18]. It requires an extended amount of applied pressure to extrude which eventually negatively affects the cell viability [25]. Therefore, we have analyzed the effect of viscosity on the transition distance by controlling the weight percentage of the solid content of the hydrogels.

2. PREPARATION OF 3D BIOPRINTER-READABLE FILE

We used a three-axis 3D bioprinter, BioX (CELLINK, Boston, MA), to fabricate the scaffold. The prepared hybrid hydrogels are stored in disposal syringes and extruded pneumatically through the same nozzle on a stationary build plane. Various printing parameters such as nozzle's internal diameter, applied air pressure, print head speed, and the perpendicular distance between the nozzle tip and print bed i.e. print distance can control the deposition rate of the material. The nozzle diameters, print speed, air pressure, and perpendicular distance between the nozzle tip and print bed used in fabricating the scaffold are respectively 410 µm, 10 mm/s, 50 kPa, and 0.405mm. Rhino 6.0 (https://www.rhino3d.com), a computer-aided design (CAD) software, is used to design and define the vectorized toolpath of a scaffold. Slicer (https://www.slicer.org), a G-code generator software is used to generate a Bio-X compatible file including the toolpath coordinates and all process parameters to fabricate the scaffold. The material is deposited in a layer-upon-layer fashion. The physical cross-linking of the fabricated scaffold after the print was ensured by the spray of $CaCl_2$. The overall scaffold fabrication process is schematically shown in Figure 1.

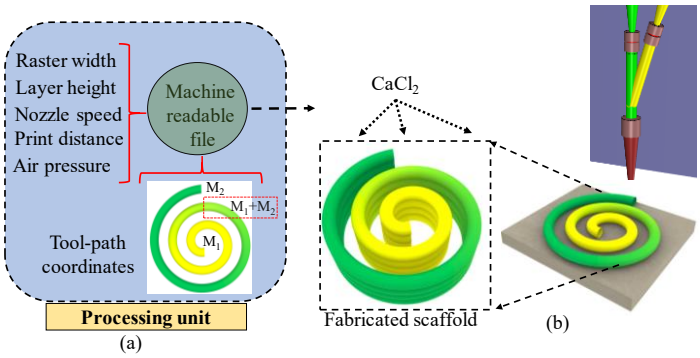

FIGURE 1: (a) Preparing machine-readable file and (b) Execution of 3D fabrication.

3. INTERCHANGEABLE NOZZLE SYSTEM DESIGN

3.1 Initial design

The initial prototype was created by running tubing through a hollowed out 3ml syringe and into a 410 µm nozzle. The syringe and nozzle were sealed with epoxy resin shown in Figure 2(a). Although we were able to extrude biomaterial, it required a substantial amount of pressure to achieve the desired results. Tubing had to be small enough to fit into the nozzle. To improve the initial prototype, we designed a set of inserts instead of tubing to allow more of the syringe volume to be filled with material. Using tubing wasted a lot of space inside the syringe, so we designed inserts that allowed to utilize more space. All the prototypes were fabricated using a Stratasys Dimension 1200es 3D printer. One prototype is shown in Figure 2(c)(i). This system took approximately 120kPa pressure that is relatively less than the initial prototype. Since the insert was 3D printed, the desired diameter of the extrusion hole was not achieved. Moreover, its inner surface was rough due to the staircase effect. This may hinder the smooth flow of the hydrogel material and eventually increase the required pressure. Another insert was designed and fabricated as shown in Figure 2(c)(ii) to separate the material into the dispensing syringe reducing the total contact surface between nozzle wall and material. This prototype was tested using the Cellink BioX 3D bioprinter by extruding various hydrogel materials such as CELLINK starter ink and a composition with 6% alginate and 6% CMC. Scaffolds fabricating with 6% alginate and 6% CMC shown in Figure 3(a). This prototype showed promising results with some adjustments. There was an issue of backflow where instead of extruding material, the pressure from one side of the system pushed the material into the other side of the system. To correct this issue, another setup was prepared including check valves. After adding check valves, the pressure would build up in the system which caused the material to continue to deposit after the pressure had been shut off. The system was also very difficult to clean. All these challenges led to the development of the current system being tested.

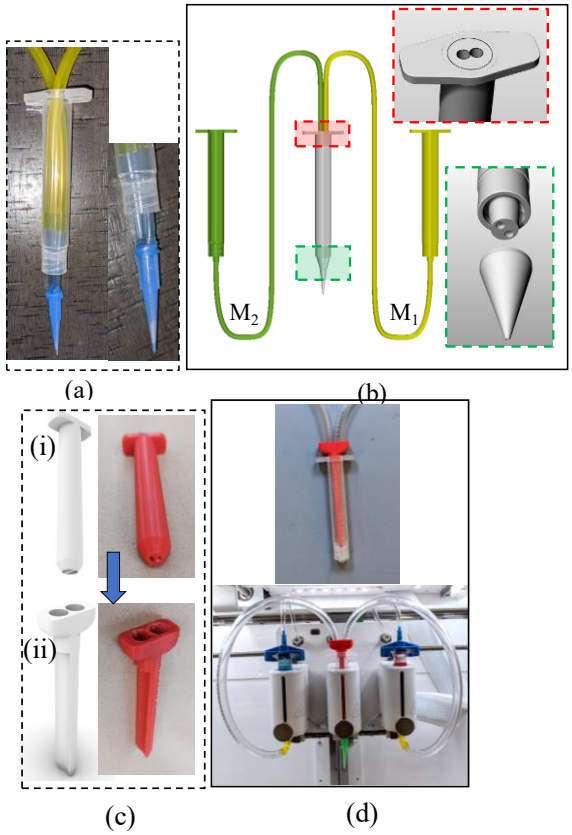

FIGURE 2: Progression of the nozzle system design process: (a) Inserting two tubes into dispensing nozzle, (b) Computer aided design of the nozzle system, (c) 3D printed inserts having two material flow system, and (d) Fabricating scaffold with 3D printed attachment.

3.2 Final design

Prototypes of the nozzle system designed and fabricated as shown in Figure 2 motivated us to design a robust nozzle system that will be easier to build, clean, and control and will require less pressure to extrude. To build such a nozzle system, we used a medical-grade Y-connector with two female Leur-lock inputs and a single male Leur-lock output (Qosina, Ronkonkoma, NY). Duckbill check valves (Qosina, Ronkonkoma, NY) are attached to the female ends of the Y-connector with the other ends connected to 3ml dispensing syringes (EFD, Nordson, East Province, RI). The entire nozzle system is shown in Figure 4(a). Dispensing nozzles are connected separately with two different printheads of the BioX 3D printer. Having a free-spinning male Leur-lock on the output of the Y-connector allows the system to be used interchangeably with any nozzle size and type. The final nozzle setup with the printer is shown in Figure 4(b). Various scaffolds with different geometries and infill densities (50-60%) having eight layers were fabricated using this designed nozzle system shown in Figure 3(b). Each bilayer was fabricated with yellow and green colored material (the composition of 6% alginate and 6% CMC was separated by yellow and green food color). The scaffold demonstrates good shape fidelity. Shape fidelity of the fabricated filament was assessed with respect to the designed filament width. Since the nozzle size used in this paper was 410 µm, we observed around 35% deviation of the filament width with respect to 410 µm. However, this deviation may vary depending on the material viscosity, applied pressure, and print distance [19]. To investigate the effectiveness of this insert, scaffold having a different internal geometry was fabricated shown in Figure 3(c-d). All fabricated scaffolds were submerged into $CaCl_2$ for 2-3 minutes to crosslink them.

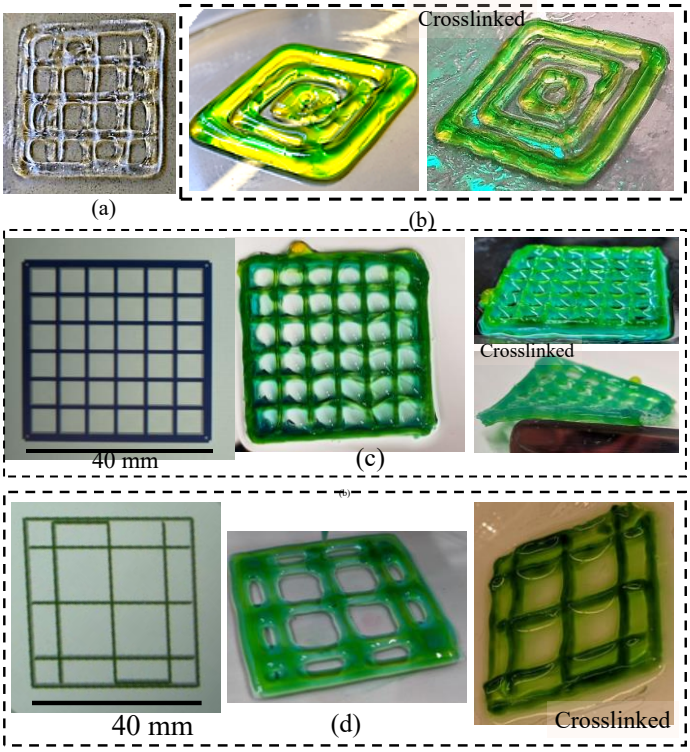

FIGURE 3: Scaffold (a) fabricated with insert shown in Figure 1(c)(ii) with composition 6% alginate-6% CMC, (b-D) fabricated with our proposed nozzle system with two different materials, and crosslinked after fabrication.

A scaffold of spiral shape was fabricated with two different materials (the composition of 6% alginate and 6% CMC was separated by yellow and green food color) shown in Figure 4(b). It required approximately 50kPa which is significantly less pressure than the previous prototypes. A comparison of required pressure of the proposed nozzle system with respect to the prototypes shown in Figure 2 is shown in Table 1.

TABLE 1: Percentage of reduction of required pressure of the proposed nozzle system with respect to the prototypes shown in Figure 2.

	Prototypes		
	1	2	3
Required Pressure (kPa) for prototype	120	100	80
Required Pressure (kPa) for proposed	50	50	50
% reduction of required pressure	140	100	60

4. VALIDATION OF THE NOZZLE SYSTEM

4.1 Hydrogel preparation

The biomaterials used for our nozzle system verification and scaffold fabrications were alginate (alginic acid sodium salt from brown algae; Sigma-Aldrich, St. Louis, MO, USA) and low viscous carboxymethyl cellulose (CMC) (pH: 6.80) (Sigma-Aldrich). Alginate is a highly used biopolymer, composed of (1-4)-linked β-Dmannuronic (M) and α-Lguluronic acids (G). This material is soluble into water, because it is negatively charged linear copolymer (M and G blocks). It also supports cell growth and exhibits high biocompatibility. Carboxymethylcellulose (CMC), a derivative of cellulose, is also water-soluble biopolymer. This copolymer is formed by two monomers such as, β-D-glucose and β-D-glucopyranose-2-O-(carboxymethyl)-monosodium salt which is connected via β-1,4-glucosidic bonds [20]. This material and is widely used as a thickener and it is non-toxic and non-allergenic [21]. Various weight percentages of alginate and CMC were used to prepare five different hybrid hydrogel samples maintaining the total solid content 8% (w/v) shown in Table 2. Food colors were used to differentiate the compositions. To mix the solution uniformly, a magnetic stirrer was used.

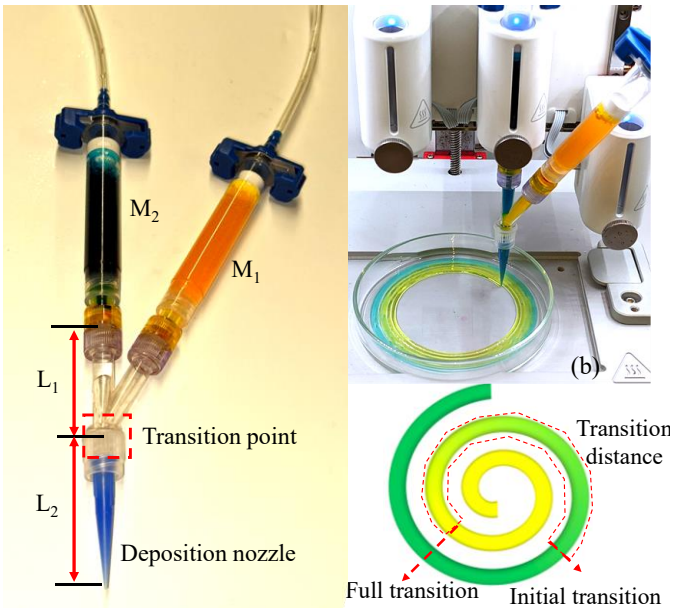

FIGURE 4: (a) Modified nozzle system, and (b) Deposition with modified nozzle system, and (c) Definition of transition distance.

TABLE 2: Composition with weight percentages.

Sample	Alginate (A) (g)	CMC (C) (g)	Alginate/CMC (%)
A_8C_0	8	0	100/0
A_6C_2	6	2	75/25
A_4C_4	4	4	50/50
A_2C_6	2	6	25/75
A_0C_8	0	8	0/100

4.2 Rheological experiment

To validate our designed nozzle system, we used a set of biomaterial compositions shown in Table 1 with different rheological properties. To determine the rheological properties of all the hydrogel compositions, we used a rotational rheometer (MCR 102, Anton Paar, Graz, Austria) with parallel plate geometry (25.0 mm flat plate). We recorded the measurements at room temperature (25^0C) with a 1.0 mm plate-plate gap. We conducted the rheological measurement at room temperature because our extrusion process is performed at room temperature, which also facilitates the quick gelation of the deposited filament [22]. The viscosities and shear stress of different concentrations were measured using a steady rate sweep test with a range of strain rate of 0.1 to 100 s^{-1}. The result of rheological properties is shown in Figure 5.

The shear-thinning properties, i.e., the phenomenon of reducing the viscosity with increasing the shear strain on hydrogels, is crucial for extruding material through a smaller diameter nozzle [23]. Hydrogels with higher viscosity experience higher shear stress during extrusion through a nozzle, which adversely affects the encapsulated cell. Viscosity is measured for all the hybrid hydrogels shown in table 1 with respect to various shear strain rates. Viscosity decreases with increasing the shear strain rate, that indicates all five compositions have shear thinning properties shown in Figure 5. Pure 8% alginate showed the lowest viscosity. The viscosity increases when the percentage of CMC into the composition is increased. However, at shear strain rate of 1.0 s^{-1}, A_2C_6 showed the highest viscosity. This composition may create the highest number of hydrogen and polar bonds due to more easily accessible bond sites of polar carbonyl groups ($C^{\delta+} = O^{\delta-}$) which drives toward a high rate of cross-linking.

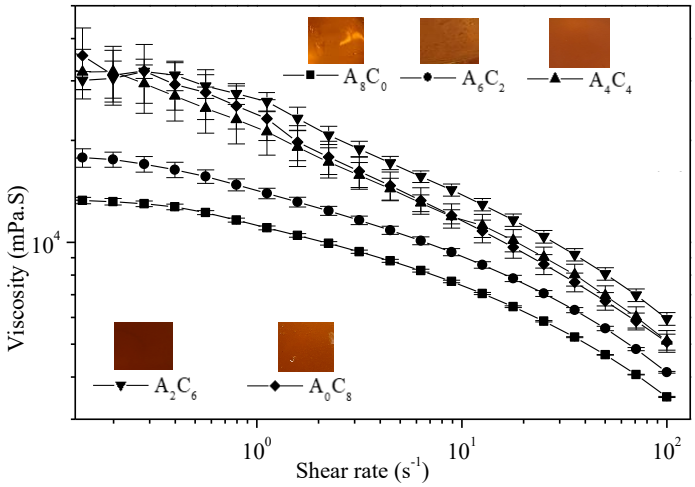

FIGURE 5: Viscosity result of different compositions.

4.3 Measuring transition distance

To determine the transition distance, we started to extrude material 2 (blue color, M2) when the extrusion nozzle was full of material 1 (yellow color, M1). We defined the event as "initial transition" when the color started to turn into blue from yellow. Finally, when the extruded material turned fully to blue, the event was defined as "Full transition". The distance between the initial transition and full transition was defined as "transition distance". All events and transition distance are schematically shown in Figure 4 (c).

A spiral toolpath is designed having a starting and ending diameter of 80mm and 2mm respectively, with 20 turns using Rhino 6 CAD software as shown in Figure 6, although printing was stopped after full transition, so the entire spiral was not printed. The proposed nozzle system was used to extrude all five types of hybrid hydrogels to fabricate that spiral scaffold. Before printing, material from one of the syringes was extruded until it filled the whole nozzle system. The other syringe was then used to print the spiral and the amount of time it took for the color to initially appear as well as to fully transition were recorded in seconds, which is shown in Figure 6. Times were multiplied by the print speed to calculate the distance of the initial color change and the full color change. The difference between the initial and full color changes was used to determine the transition difference. To save time, two different printing programs were set up, one using the first tool for extrusion and the other using the third tool. This allowed us to easily switch between the two

each time instead of having to extrude the second material before each print. A minimum of five trials (n=5) was conducted with each concentration of biomaterial maintaining all other parameters as constant. This calculated information from each of the trials was used to find the average initial transition distance, average full transition distance, and average difference distance for each concentration tested. We presented all the data in a form of mean ± standard deviation. To assess the statistical significance of differences in transition distance, we considered the distribution of values is normal. A two-way ANOVA and a significance level of p = 0.05 were used to determine the statistically significant differences. Minitab18.0 and OriginPro 5.0 two statistical software were used to do the quantitative and graphical analysis.

Figure 7(a) represents the initial, full, and actual transition distances separately. Figure 7(b) shows them stacked so that the total transition information can be seen. The second in this figure is quite important for this experiment, because the best concentration will ultimately be the one with the shortest transition distance for all three categories. Based on the data collected, A_6C_2 has the shortest transition distance for all three categories, making it the best overall concentration for this system. With A_6C_2, the initial transition and full transition distances increase as the percent of CMC increases and percent alginate decreases. This is most likely due to the thickening properties or the viscosity increase. Surprisingly, the trend is not consistent with A_8C_0, indicating CMC must have some benefit in small concentrations or alginate on its own is more sticky than viscous. The initial transition is also mostly viscosity dependent except A_8C_0. Therefore, a small portion of CMC is likely increasing the followability and eventually assists the material transition better where a larger proportion of CMC, i.e., high-viscous hydrogel, can create difficulty with smooth transition in a single nozzle deposition system.

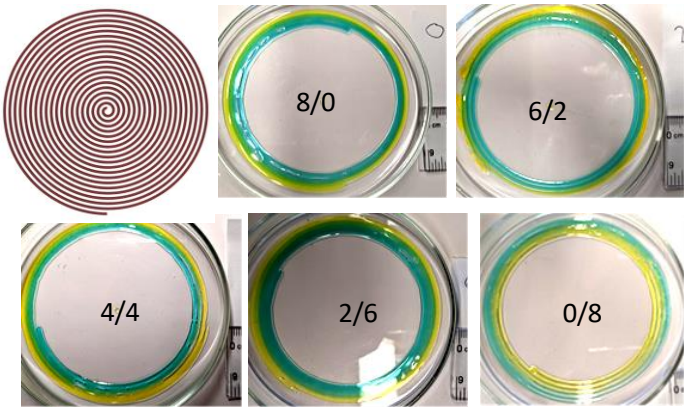

FIGURE 6: Determining transition distance of various compositions.

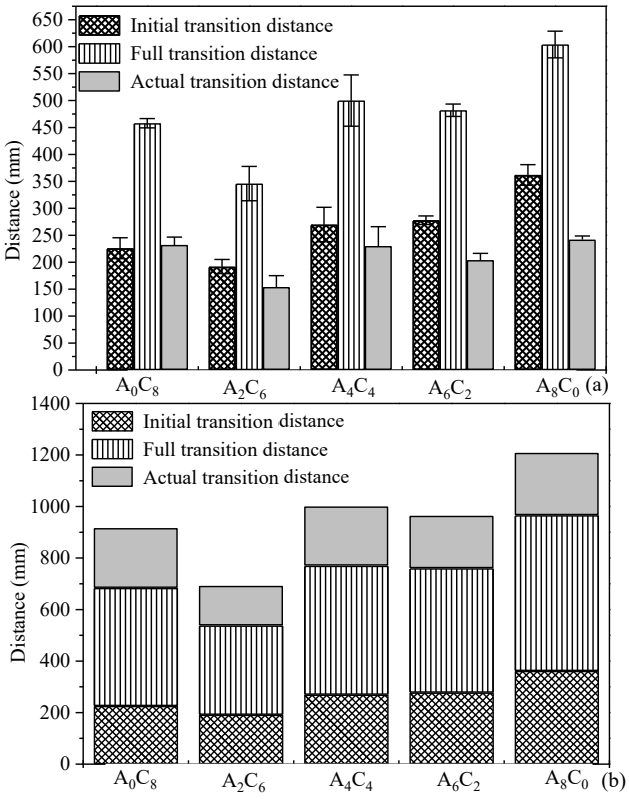

FIGURE 7: Transition distances of various compositions.

5. DISCUSSION

Hydrogels prepared with various polymers extracted from nature, such as alginate, collagen, gelatin, chitosan, and cellulose, etc., were successfully used for bioprinting [24-26]. However, achieving the printability and maintaining the shape fidelity of the 3D printed scaffold with a great spatial control are still challenging [22, 27]. Attempting to bioprint with multiple biomaterials ensuring material transition, scaffold geometry, and good cell viability adds more roadblocks toward a successful tissue fabrication [2]. An interchangeable nozzle system with easy material transition and less required pressure can offer a good solution. Therefore, a nozzle system which is easier to build, clean and control the material transition was designed, built and validated in this paper. It also requires less pressure to extrude which will provide protection for encapsulated cells during extrusion and eventually good cell viability. Moreover, this system can extrude materials with various viscosities. The addition of co-axial nozzles with this interchangeable system can help the scaffold fabrication with vascularity and a successful tissue fabrication in long run. A conical structure including three materials supply system with a common intersection to extrude the material can help add more variation with the proposed system. The effect of the material viscosity on various transition scenarios was analyzed with our proposed nozzle system. If the initial or full distance is too large, it will be more challenging to time the transition in a real scaffold bioprint. Even when the initial transition is very small, if the transition difference is too

large, the deposition will not be precise enough for functional tissue or any type of bioprint. A large transition difference could be useful when printing functional gradients, but that is not the goal of this research. An interconnected system ensuring crosstalk between the hardware and software systems to manage the user-defined fabrication recipe is on-going in our research. The future direction of this research is to use a surface modifier such as a superhydrophobic coating in the Y-connector to assist in smooth material transition. Moreover, controlling the overall length L (L_1+L_2), using a dispensing nozzle with a shorter length, can reduce the transition distance, which will also be analyzed in the future. Finally, various hydrogels encapsulating multiple cells will be extruded and analyzed to validate this proposed nozzle system.

6. CONCLUSION

We have demonstrated the development of an interchangeable nozzle system for 3D bio-printing technique to fabricate scaffolds with multiple hydrogels. The proposed nozzle system can interchange the deposition of multiple hydrogels smoothly through a single nozzle. This system allows the deposition and transition of hydrogels having various viscosities. It is believed that further improvements of this proposed interchangeable nozzle system will contribute to enhancing the ability to fabricate scaffolds having complex internal and external geometry. In the long run this system will help fabricate multiple cell encapsulated hydrogels to regenerate the tissue construct.

ACKNOWLEDGEMENTS

Research was supported by New Hampshire-EPSCoR through BioMade Award #1757371 from National Science Foundation and New Hampshire-INBRE through an Institutional Development Award (IDeA), P20GM103506, from the National Institute of General Medical Sciences of the NIH.

REFERENCES

1. Ahn, S., H. Lee, and G. Kim, *Functional cell-laden alginate scaffolds consisting of core/shell struts for tissue regeneration.* Carbohydrate polymers, 2013. **98**(1): p. 936-942.
2. Wang, Z., et al., *3D bioprinted functional and contractile cardiac tissue constructs.* Acta biomaterialia, 2018. **70**: p. 48-56.
3. Kong, H.-J., K.Y. Lee, and D.J. Mooney, *Decoupling the dependence of rheological/mechanical properties of hydrogels from solids concentration.* Polymer, 2002. **43**(23): p. 6239-6246.
4. Markstedt, K., et al., *3D bioprinting human chondrocytes with nanocellulose–alginate bioink for cartilage tissue engineering applications.* Biomacromolecules, 2015. **16**(5): p. 1489-1496.
5. Kolesky, D.B., et al., *Three-dimensional bioprinting of thick vascularized tissues.* Proceedings of the National Academy of Sciences, 2016. **113**(12): p. 3179-3184.
6. Bertassoni, L.E., et al., *Hydrogel bioprinted microchannel networks for vascularization of tissue engineering constructs.* Lab on a Chip, 2014. **14**(13): p. 2202-2211.
7. Zhang, Y.S., et al., *Bioprinting 3D microfibrous scaffolds for engineering endothelialized myocardium and heart-on-a-chip.* Biomaterials, 2016. **110**: p. 45-59.
8. Nadernezhad, A., et al., *Multifunctional 3D printing of heterogeneous hydrogel structures.* Scientific reports, 2016. **6**(1): p. 1-12.
9. Shim, J.-H., et al., *Bioprinting of a mechanically enhanced three-dimensional dual cell-laden construct for osteochondral tissue engineering using a multi-head tissue/organ building system.* Journal of Micromechanics and Microengineering, 2012. **22**(8): p. 085014.
10. Xu, T., et al., *Hybrid printing of mechanically and biologically improved constructs for cartilage tissue engineering applications.* Biofabrication, 2012. **5**(1): p. 015001.
11. Kundu, J., et al., *An additive manufacturing-based PCL–alginate–chondrocyte bioprinted scaffold for cartilage tissue engineering.* Journal of tissue engineering and regenerative medicine, 2015. **9**(11): p. 1286-1297.
12. Miri, A.K., et al., *Microfluidics-enabled multimaterial maskless stereolithographic bioprinting.* Advanced Materials, 2018. **30**(27): p. 1800242.
13. Sakai, S., et al., *Drop-On-Drop Multimaterial 3D Bioprinting Realized by Peroxidase-Mediated Cross-Linking.* Macromolecular rapid communications, 2018. **39**(3): p. 1700534.
14. Ruiz-Cantu, L., et al., *Multi-material 3D bioprinting of porous constructs for cartilage regeneration.* Materials Science and Engineering: C, 2020. **109**: p. 110578.
15. Sodupe-Ortega, E., A. Sanz-Garcia, and C. Escobedo-Lucea, *Accurate calibration in multi-material 3D bioprinting for tissue engineering.* Materials, 2018. **11**(8): p. 1402.
16. Kolesky, D.B., et al., *3D bioprinting of vascularized, heterogeneous cell-laden tissue constructs.* Advanced materials, 2014. **26**(19): p. 3124-3130.
17. Maiullari, F., et al., *A multi-cellular 3D bioprinting approach for vascularized heart tissue engineering based on HUVECs and iPSC-derived cardiomyocytes.* Scientific Reports, 2018. **8**(1): p. 13532.
18. Hardin, J.O., et al., *Microfluidic printheads for multimaterial 3D printing of viscoelastic inks.* Advanced materials, 2015. **27**(21): p. 3279-3284.
19. Habib, A., et al., *3D printability of alginate-carboxymethyl cellulose hydrogel.* Materials, 2018. **11**(3): p. 454.

20. Han, Y. and L. Wang, *Sodium alginate/carboxymethyl cellulose films containing pyrogallic acid: physical and antibacterial properties.* Journal of the Science of Food and Agriculture, 2017. **97**(4): p. 1295-1301.
21. Tongdeesoontorn, W., et al., *Effect of carboxymethyl cellulose concentration on physical properties of biodegradable cassava starch-based films.* Chemistry Central Journal, 2011. **5**(1): p. 6.
22. Ouyang, L., et al., *Effect of bioink properties on printability and cell viability for 3D bioplotting of embryonic stem cells.* Biofabrication, 2016. **8**(3): p. 035020.
23. Li, H., et al., *3D bioprinting of highly thixotropic alginate/methylcellulose hydrogel with strong interface bonding.* ACS applied materials & interfaces, 2017. **9**(23): p. 20086-20097.
24. Abouzeid, R.E., et al., *Biomimetic mineralization of three-dimensional printed alginate/TEMPO-oxidized cellulose nanofibril scaffolds for bone tissue engineering.* Biomacromolecules, 2018. **19**(11): p. 4442-4452.
25. Di Giuseppe, M., et al., *Mechanical behaviour of alginate-gelatin hydrogels for 3D bioprinting.* Journal of the mechanical behavior of biomedical materials, 2018. **79**: p. 150-157.
26. Diamantides, N., et al., *Correlating rheological properties and printability of collagen bioinks: the effects of riboflavin photocrosslinking and pH.* Biofabrication, 2017. **9**(3): p. 034102.
27. Chung, J.H., et al., *Bio-ink properties and printability for extrusion printing living cells.* Biomaterials Science, 2013. **1**(7): p. 763-773.